



Chinese Society of Aeronautics and Astronautics  
& Beihang University

Chinese Journal of Aeronautics

cja@buaa.edu.cn  
www.sciencedirect.com



# Motion synchronization in a dual redundant HA/EHA system by using a hybrid integrated intelligent control design



Waheed Ur Rehman, Wang Shaoping, Wang Xingjian\*, Fan Lei, Kamran Ali Shah

School of Automation Science and Electrical Engineering, Beihang University, Beijing 100191, China

Received 10 August 2015; revised 25 September 2015; accepted 8 October 2015

Available online 22 December 2015

## KEYWORDS

Dissimilar redundant;  
Electro-hydrostatic actuator;  
Fuzzy control;  
Hydraulic actuator;  
Motion synchronization;  
Redundant systems

**Abstract** This paper presents an integrated fuzzy controller design approach to synchronize a dissimilar redundant actuation system of a hydraulic actuator (HA) and an electro-hydrostatic actuator (EHA) with system uncertainties and disturbances. The motion synchronous control system consists of a trajectory generator, an individual position controller for each actuator, and a fuzzy force tracking controller (FFTC) for both actuators. The trajectory generator provides the desired motion dynamics and designing parameters of the trajectory which are taken according to the dynamic characteristics of the EHA. The position controller consists of a feed-forward controller and a fuzzy position tracking controller (FPTC) and acts as a decoupled controller, improving position tracking performance with the help of the feed-forward controller and the FPTC. The FFTC acts as a coupled controller and takes into account the inherent coupling effect. The simulation results show that the proposed controller not only eliminates initial force fighting by synchronizing the two actuators, but also improves disturbance rejection performance.

© 2015 The Authors. Production and hosting by Elsevier Ltd. on behalf of Chinese Society of Aeronautics and Astronautics. This is an open access article under the CC BY-NC-ND license (<http://creativecommons.org/licenses/by-nc-nd/4.0/>).

## 1. Introduction

The reliability requirements of large aircraft are increasingly high, so conventional flight control systems adopt similar

redundant hydraulic actuators with central hydraulic power supply systems. Hydraulic actuators (HAs) have very good characteristics such as small size-to-power ratio and ability to provide large torque and force.<sup>1–3</sup> However, this configuration is difficult to further enhance aircraft reliability because of their heavy reservoirs, long pipes, and other necessary accessories. In order to improve aircraft reliability and maintainability, A380 firstly develops a dissimilar redundant actuation configuration based on an HA and an electro-hydrostatic actuator (EHA).<sup>4</sup> Since the EHA is a distributed electro-hydrostatic actuation system, in which an electrical motor acts as the control unit and a hydraulic pump works as the transmission part, its dynamic performance is totally

\* Corresponding author. Tel.: +86 10 82338917.

E-mail addresses: [wrehman87@gmail.com](mailto:wrehman87@gmail.com) (W. Ur Rehman), [shaopingwang@vip.sina.com](mailto:shaopingwang@vip.sina.com) (S. Wang), [wangxj@buaa.edu.cn](mailto:wangxj@buaa.edu.cn) (X. Wang).

Peer review under responsibility of Editorial Committee of CJA.



Production and hosting by Elsevier

different from that of the HA.<sup>5</sup> The EHA takes advantage of electric technology, including environmental cleanliness, energy saving, and reduced hydraulic pipes.<sup>6–8</sup> Therefore, in the dissimilar redundant actuation system, the HA/EHA is the best option for an application that needs high force and requires high fault tolerance capability.<sup>9–11</sup>

Although the dissimilar redundant actuation system not only reduces weights but also improves maintainability with segregating power distribution channels, its control faces a challenge because of the different dynamic performances between the HA and the EHA.<sup>12</sup>

There are two operating modes for the dissimilar redundant actuation system, i.e., HA active/EHA active (A/A) mode and HA active/EHA passive (A/P) mode.<sup>13</sup> Most aircraft use the A/P mode, but there are certain circumstances, such as sudden storms or actuator failure, that demand the A/A mode.<sup>14</sup> The HA and the EHA are connected to the control surface through a rigid connection, in which these two actuators have different driving principles. The coupling effect that is due to the rigid connection between them produces force fighting. Force fighting is the amount of force difference between the HA and the EHA, which not only disturbs tracking accuracy, but also can damage the control surface.<sup>15</sup> Therefore, how to control force fighting by taking the inherent coupling effect into account is a hot topic for modern aircraft.

In order to check and analyze the performance of the dissimilar redundant actuation system, a test bench of the hybrid system has been built by GOODRICH Company and INSA University.<sup>13,16</sup> Two strategies have been given. One strategy uses an active mode without load, in which the actuator position difference, velocity difference, and force difference are used by a position controller to synchronize them. The other strategy uses a multiple-input multiple-output (MIMO) control method based on a state observer to reduce force fighting.<sup>17</sup> The difference between the average actuator force and the actual actuator force is given to the integrator to generate a position demand offset for eliminating force fighting.<sup>10</sup> Different techniques for static force equalization and dynamic force equalization have been studied,<sup>10,15,18</sup> but there is a flaw in the above techniques because they seldom consider their coupling effect. In fact, it is the mutual coupling between the HA and the EHA that is the key to restrict its dynamic performance.

In order to improve the tracking performance of the hybrid system, the coupling effect should be taken into account. Motion synchronization can guarantee the elimination of force fighting. With the purpose of reducing the force fighting effect between different channels, a robust adaptive fuzzy method that takes the coupling term through T–S fuzzy is proposed for a multi-input and multi-output system.<sup>19,20</sup> An adaptive fuzzy sliding mode controller is designed for a two-joint manipulator and every joint can realize high precision tracking control by using fuzzy terminal sliding mode control.<sup>21</sup> Robust control theory is used to solve the coupling problem by taking coupling as disturbance between different channels and a synchronous controller is designed with the help of quantized field theory (QFT).<sup>22,23</sup> An adaptive PID controller is used for speed control of a permanent magnetic synchronous motor.<sup>24,25</sup>

However, the above literatures only focus on the coupling effect and not investigating the source of coupling between the HA and the EHA. In addition, the controller design doesn't consider the system uncertainties and disturbances. This paper presents an integrated fuzzy controller based on a

trajectory generator, a piston controller, and a fuzzy force tracking controller (FFTC). The trajectory generator provides the desired motion dynamics (position, velocity, acceleration) and the designing parameters of the trajectory are taken according to the dynamic characteristics of the EHA. The position controller consists of a feed-forward controller and a fuzzy position tracking controller (FPTC) and acts as a decoupled controller, improving position tracking performance with the help of the feed-forward controller and the FPTC. The FFTC acts as a coupled controller and takes into account the inherent coupling effect to synchronize two actuators and improve disturbance rejection performance. Through trajectory control, position decoupling control, and force tracking control, the dissimilar redundant actuation system can approach desired dynamics, reduce the position tracking error caused by disturbances and nonlinearities, and improve the load rejection performance through taking into account the inherent coupling effect between the HA and the EHA. The simulation results illustrate that the proposed controller is effective to eliminate initial force fighting and to improve disturbance rejection performance.

## 2. Mathematical modeling of the dissimilar redundant actuation system

The structure of the dissimilar redundant actuation system is shown in Fig. 1, which consists of an EHA (combination of a motor, a pump, and a hydraulic cylinder), an HA (combination of a servo valve and a hydraulic cylinder), and a control surface. The pilot gives the command to a flight control computer which drives the servo valve of the HA and the motor of the EHA respectively.

In Fig. 1,  $F_h$  and  $F_e$  are the output forces of the HA and the EHA, respectively, while  $F_l$  is an equivalent air load force.

Since some nonlinear factors exist in the HA and the EHA, the dynamic performance of the HA is different from that of the EHA. In addition, the disturbance around the dissimilar actuation system will also influence the dynamic performances of the HA and the EHA. Therefore, there are some differences between the HA and the EHA, leading to the force fighting act on the control surface. If the force fighting acts on the surface continuously, it may result in damage of the control surface. Therefore, it is necessary to figure out the reasons of the force fighting and find a solution to eliminate the force fighting effectively for satisfying maneuvering performance. In order to analyze the dynamic performance of the whole system, it needs to drive mathematical models of the HA, the EHA, and the control surface.

### 2.1. Mathematical models of the actuators

#### 2.1.1. HA modeling

The HA includes a hydraulic power supply system, a servo valve, a cylinder, and a displacement sensor, as shown in Fig. 1. The mathematical model of the HA is derived according to the displacement and load flow of the servo valve. In order to derive a mathematical model of the HA, the nonlinearities are ignored. Suppose that the spool displacement of the servo valve is linearly related to the servo valve current and the flow of the servo valve is linear around null opening to the servo valve current and load pressure as follows:

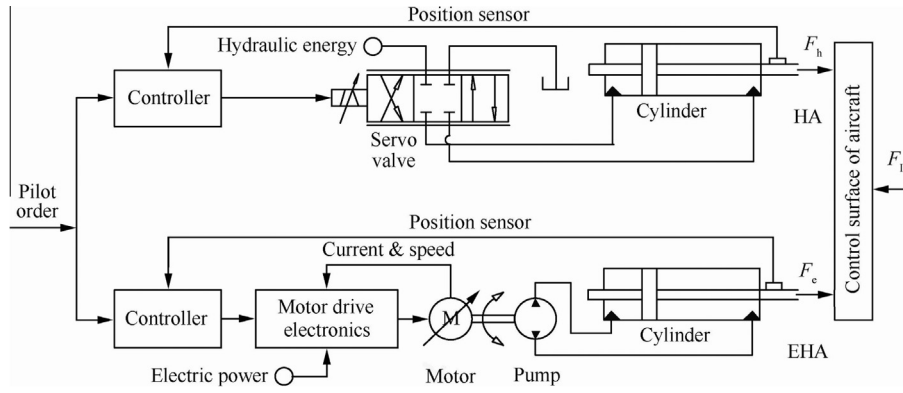


Fig. 1 Structure of the dissimilar redundant actuation system.

$$\begin{cases} \dot{x}_v = K_i I_s \\ Q_h = K_q x_v - K_c P_h \end{cases} \quad (1)$$

where  $x_v$  is the spool displacement of the servo valve;  $K_i$  is the opening/current gain of the servo valve;  $I_s$  is the input current of the servo valve;  $Q_h$  is the flow of the servo valve;  $K_q$  is the flow/opening gain at null pressure drop of the servo valve;  $K_c$  is the servo valve flow/pressure gain;  $P_h$  is the load pressure of the servo valve.

The flow dynamics and force dynamics of the cylinder can be described by:

$$\begin{cases} Q_h = A_h \dot{x}_h + \frac{V_h}{4E_h} \dot{P}_h + C_{hl} P_h \\ A_h P_h = m_h \ddot{x}_h + B_h \dot{x}_h + F_h \end{cases} \quad (2)$$

where  $A_h$  is the piston area;  $x_h$  is the displacement of the cylinder;  $V_h$  is the total volume of the cylinder;  $E_h$  is the effective bulk modulus;  $m_h$  is the mass of the hydraulic cylinder rod;  $B_h$  is the viscous resistance in the hydraulic cylinder;  $C_{hl}$  is the leakage coefficient.

Combine Eqs. (1) and (2) to obtain the block diagram of the HA shown in Fig. 2, in which  $K_{ce} = C_{hl} + K_c$  is the total leakage coefficient.

### 2.1.2. EHA modeling

The EHA consists of a motor, a hydraulic pump, a cylinder, a displacement sensor, and a control surface, as shown in Fig. 1. In order to derive a mathematical model of the EHA, the nonlinearities are ignored. The dynamics of the pump controlled motor in the form of voltage balance, torque balance, and load torque equation are given as

$$\begin{cases} U_e = K_e \omega_e + L_e \frac{d i_e}{dt} + R_e i_e \\ K_m i_e = T_e + J_m \dot{\omega}_e + B_m \omega_e \end{cases} \quad (3)$$

where  $U_e$  is the applied voltage inputting to the EHA;  $K_e$  is the back-EMF constant;  $\omega_e$  is the angular velocity;  $L_e$  is the armature inductance;  $R_e$  is the armature resistance;  $i_e$  is the motor

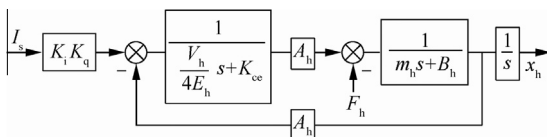


Fig. 2 Block diagram of the HA.

current;  $K_m$  is the electromagnetic torque constant;  $J_m$  is the inertia of the rotor and the shaft;  $B_m$  is the total damping between the motor and the shaft;  $T_e = V_p P_e$  is the load torque on the shaft, in which  $V_p = V/2\pi$ , where  $V$  is the pump displacement, and  $P_e$  is the load pressure.

For the hydraulic cylinder of the EHA, the flow dynamics and force dynamics can be described by:

$$\begin{cases} Q_e = A_e \dot{x}_e + \frac{V_e}{4E_e} \dot{P}_e + C_{el} P_e \\ A_e P_e = m_e \ddot{x}_e + B_e \dot{x}_e + F_e \end{cases} \quad (4)$$

where  $Q_e = V_p \omega_e$  is the output flow of the pump;  $A_e$  is the effective area of the hydraulic cylinder piston;  $x_e$  is the output displacement of the EHA;  $V_e$  is the total volume of the hydraulic cylinder;  $E_e$  is the effective bulk modulus;  $C_{el}$  is the total leakage factor;  $m_e$  is the mass of the hydraulic cylinder rod;  $B_e$  is the viscous resistance in the hydraulic cylinder.

Let  $B_{me} = K_e K_m / R_e + B_m$  and combine Eqs. (3) and (4) to obtain the block diagram of the EHA as shown in Fig. 3, where the armature inductance is ignored because of its very small value compared with that of the armature resistance.

### 2.2. Mathematical model of the control surface

Suppose that the actuators are rigidly connected to the control surface and the movement angle  $\theta_d$  of the control surface is not large and equal to the linear movement  $x_d$  of the control surface, i.e.,  $\theta_d = x_d/r_d$ , where  $r_d$  is the radial distance of the control surface. The structure of the control surface driven by the hydraulic cylinder is shown in Fig. 4.

The force dynamics of the aircraft control surface can be given as

$$F_h + F_e = m_d \ddot{x}_d + B_d \dot{x}_d + F_L + K_d x_d \quad (5)$$

where  $K$  is the transmission stiffness;  $m_d$  is the mass of the control surface;  $B_d$  is the viscous damping coefficient;  $K_d$  is the aero elasticity.  $F_h$  and  $F_e$  can be described by:

$$\begin{cases} F_h = K(x_h - x_d) \\ F_e = K(x_e - x_d) \end{cases} \quad (6)$$

### 2.3. Force fighting analysis

Due to different stiffness properties, tolerances, and components, the force fighting on the shaft exists between the HA

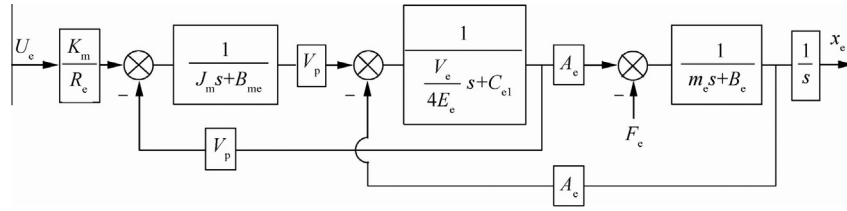


Fig. 3 Block diagram of the EHA.

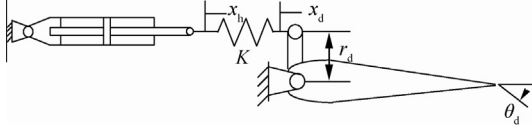


Fig. 4 Driving mechanism of the control surface.

and the EHA in the dissimilar redundant actuation system. The dynamic force fighting is a very important issue that influences the dynamic performance of the actuation system. The force fighting can decrease the system efficiency and cause surface damage. In order to remove the dynamic force fighting, it is required that the HA and the EHA should have identical pursuit dynamics and rejection properties.

Fig. 5 shows the connection of the dissimilar redundant actuation system based on the HA and the EHA with an external load force  $F_L$ , in which the HA possesses a displacement  $x_h$  and a load force  $F_h$  and the EHA has a displacement  $x_e$  and a load force  $F_e$  under the same input.  $X_r$  is the reference input of the system.

The transfer function of the HA displacement is given by

$$x_h = \frac{X_r - G_2(s)F_h}{G_1(s)} \quad (7)$$

where  $G_1(s)$  is the input transfer function of the HA and  $G_2(s)$  is the disturbance rejection function of the HA.

The transfer function of the EHA displacement is given by

$$x_e = \frac{X_r - H_2(s)F_e}{H_1(s)} \quad (8)$$

where  $H_1(s)$  is the input transfer function of the EHA and  $H_2(s)$  is the disturbance rejection function of the EHA.

The force fighting  $e_f$  is defined as the force difference between the two actuators, and given by

$$e_f = K \left( \frac{x_r - G_2(s)F_h}{G_1(s)} - \frac{x_r - H_2(s)F_e}{H_1(s)} \right) \quad (9)$$

Eq. (9) shows that the force fighting will be zero under two conditions: (1) when  $1/G_1(s)$  and  $1/H_1(s)$  are the same (the position pursuits functions are the same); (2) when  $G_2(s)/G_1(s)$  and  $H_2(s)/H_1(s)$  are the same (the rejection functions of the actuators to external force are the same).

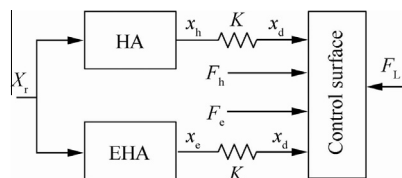


Fig. 5 Diagram of the dissimilar redundant actuation system.

### 3. Hybrid integrated intelligent control design for motion synchronization

For the dissimilar redundant actuation system, it is difficult to design a controller that can get the desired performance for the HA and the EHA due to inconsistent dynamics between the HA and the EHA. Hence, this paper presents an intelligent nested fuzzy controller shown in Fig. 6, which consists of a trajectory generator, a position controller, and an FFTC to improve load rejection performance.

In Fig. 6,  $X_{tr}$ ,  $\dot{X}_{tr}$ , and  $\ddot{X}_{tr}$  are the reference position, velocity, and acceleration of the desired trajectory profile given by the trajectory generator.  $I_{s12}$  and  $U_{e12}$  are the outputs of the position controller for the HA and the EHA, respectively.  $I_{s3}$  and  $U_{e3}$  are the outputs of the FFTC for the HA and the EHA, respectively.

#### 3.1. Trajectory generator

The desired dynamics are set by the trajectory generator. Trajectory generates three outputs as the reference position  $X_{tr}$ , velocity  $\dot{X}_{tr}$ , and acceleration  $\ddot{X}_{tr}$  by taking  $X_r$  as the reference input. The trajectory which is going to be used in this research is a second-order transfer function; it has two designing parameters, the reference frequency  $\omega_i$  and the reference damping factor  $\zeta_i$  shown in Fig. 7. These two parameters of the EHA are used in building the desired trajectory.

#### 3.2. Position controller

The position controller for the actuators consists of a feed-forward controller and an FPTC, as shown in Fig. 8.

In Fig. 8,  $I_{s1}$  and  $U_{e1}$  are the outputs of the feed-forward controller for the HA and the EHA, respectively, while similarly  $I_{s2}$  and  $U_{e2}$  are the outputs of the FPTC for the HA and the EHA, respectively. The feed-forward controller overcomes sluggish dynamics and acts in a pre-defined way while the FPTC ensures the system operate in a desired point and improves performance robustly. The position controller uses a feedback controller and a feed-forward controller together to provide a rapid response and to track the desired motion given by the trajectory generator.

##### 3.2.1. Feed-forward controller

It is a control technique that responds to disturbance in a pre-defined way. A feed-forward controller is based on prediction of plant behavior and can react before an error occurs. Therefore, it overcomes sluggish dynamics and delays in the system and also doesn't influence system stability. It has the disadvan-

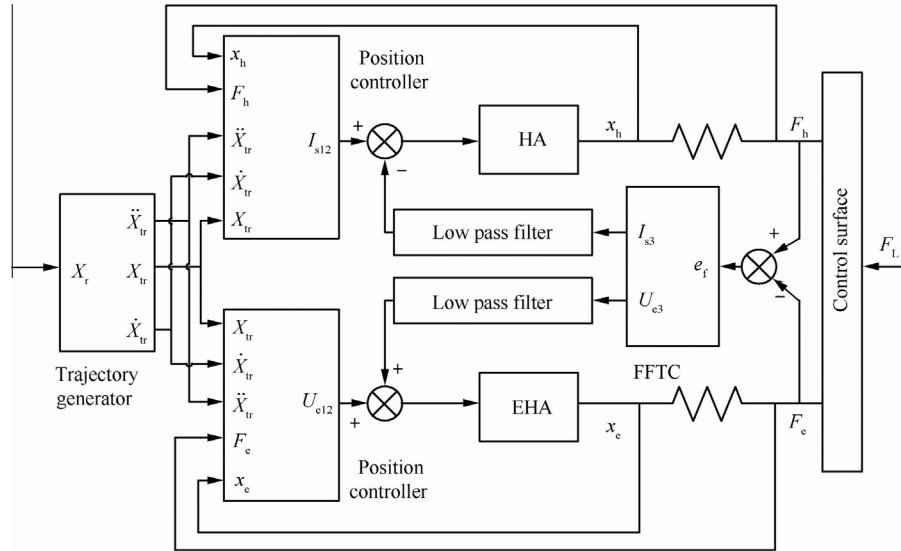


Fig. 6 Controller structure for the dissimilar redundant actuation system.

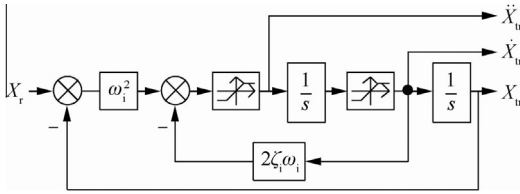


Fig. 7 Schematic of second order trajectory.

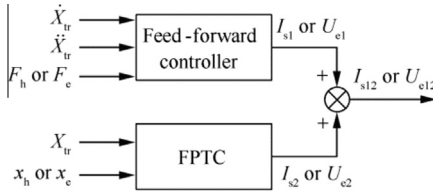


Fig. 8 Structure of the position controller.

tage that it acts against disturbance by prediction, not by measuring disturbance, so it will not be accurate enough if the system changes. A feed-forward controller ideally consists of an exact inverse model of a plant, so it can compensate for known plant dynamics, delays, and errors before they happen.

Based on the actuator model, the feed-forward controller algorithm implements the equivalent inverse dynamics by assuming that the actuator output is the desired reference trajectory. Taking the HA as an example and considering the mathematical model of the HA (i.e., Eqs. (1) and (2)), the feed-forward controller for the HA can be designed as:

$$I_{s1} = \frac{1}{K_i K_q} \left[ A_h \dot{X}_{tr} + \left( \frac{V_h}{4E_h} s + K_{cc} \right) P_h \right] \quad (10)$$

### 3.2.2. Fuzzy position tracking controller

In order to further improve position tracking control performance and to compensate for inaccuracies caused by

disturbances and nonlinearities, the FPTC is designed for each individual actuator.

The conventional PI controllers have been widely used in many applications for industrial automation and process control because of simplicity and ease of operation. Fuzzy control is a very good approach for some systems such as higher-order nonlinear systems, time-delay linear systems, and complex systems that have no precise and accurate models.<sup>26,27</sup> Considering the difficulties to get a highly precise mathematical model of the HA/EHA redundant actuation system and high position tracking performance, a hybrid fuzzy PI control approach as the FPTC is used in this paper. The structure of the fuzzy position tracking controller is shown in Fig. 9. It is just like a parallel combination in which fuzzy logic is used to tune the parameters of a PI controller.

In Fig. 9,  $e_p$  is the position tracking error.  $D_{p1}$  and  $D_{p2}$  are the gains to convert the input (position tracking error) into a form which is suitable for interfacing of the fuzzy logic controller.  $C_1$ ,  $C_2$ ,  $G_2$ , and  $G_2$  are the controller parameters needed to be adjusted.  $K'_p$  and  $K'_i$  are the turning parameters.

The fuzzy logic controller may be considered as a parallel combination in which fuzzy logic is used to tune the parameters of a PI controller, and it has four main components:

- (1) The “rule base” holds the knowledge, in the form of a set of rules as shown in Table 1, and every rule represents the states of member functions which are shown in Table 2.
- (2) The inference mechanism evaluates control rules and makes a decision.
- (3) The fuzzification interface simply modifies the input into such a form that can be easily interpreted and compared to the rules.
- (4) The defuzzification interface converts the conclusions given by the inference mechanism to the plant.

The triangular member function  $\mu_r$  will be used whose general formula is given as

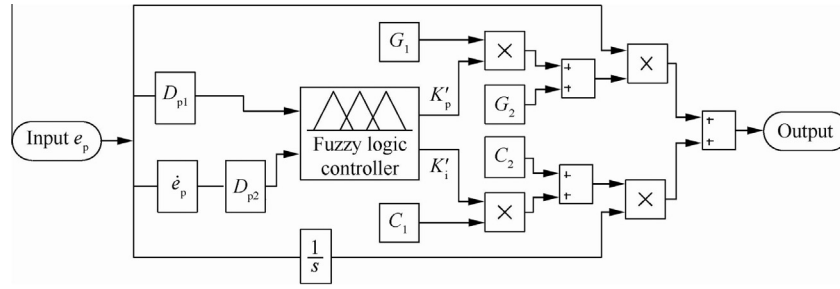


**Fig. 9** Structure of the fuzzy position tracking controller.

**Table 1** Fuzzy rules for the FPTC.

Change of error $\dot{e}_p$	Error $e_p$				
	NB	NS	ZE	PS	PB
NB	S	S	MS	MS	M
NS	S	MS	MS	M	MB
ZE	MS	MS	M	MB	MB
PS	MS	M	MB	MB	B
PB	M	MB	MB	B	B

$$\mu_r = \begin{cases} 0 & x \leq a_r \\ (x - a_r)/(b_r - a_r) & a_r < x < b_r \\ (c_r - x)/(c_r - b_r) & b_r < x < c_r \\ 0 & c_r \leq x \end{cases} \quad (11)$$

where  $r \in \{\text{NB, NS, ZE, PS, PB, S, MS, M, MB, B}\}$ .

The fuzzy rules for all tuning parameters of the FPTC is the same but their membership functions are different. The membership function for each parameter of the FPTC is given in Table 2.

Suppose that the varied ranges of parameters  $K_p$  and  $K_i$  of the FPTC are bounded. A suitable range of each parameter can be found by the simulation of the convention PI controller. The range of each parameter for the FPTC of the HA is  $K_p \in [0.82, 0.88]$  and  $K_i \in [5.20, 5.50]$ . The range of each parameter for the FPTC of the EHA is  $K_p \in [8950, 9050]$  and  $K_i \in [21, 900, 22, 100]$ . They can be calibrated by using a general formula given by

$$K_z = (K_{z \max} - K_{z \min})K'_z + K_{z \min} \quad (12)$$

where subscript  $z$  shows the type of the tuning parameter, and it may be proportional or integral.

### 3.3. Fuzzy force tracking controller

The position controller is designed to improve position tracking performance of each individual actuator. However, it does not take into account the inherent coupling effect in a hybrid redundant actuation system of HA/EHA, so the position controller can't improve load rejection performance effectively. Motion synchronization and position tracking performance are equally important in the dissimilar redundant actuation system. To address motion synchronization, an FFTC is proposed to connect two individual actuators and to synchronize motion between the HA and the EHA. The FFTC is basically a PID-type hybrid fuzzy control algorithm as shown in Fig. 10.

In Fig. 10,  $D_{f1}$  and  $D_{f2}$  are the gains to convert the input (force tracking error) into a form which is suitable for interfacing of the fuzzy logic controller.  $K'_{ph}$ ,  $K'_{ih}$ ,  $K'_{dh}$ ,  $K'_{pe}$ ,  $K'_{ie}$ , and  $K'_{de}$  are the turning parameters.  $K_{ph}$ ,  $K_{ih}$ ,  $K_{dh}$ ,  $K_{pe}$ ,  $K_{ie}$ , and  $K_{de}$  are the PID controller parameters.  $I_{s3}$  and  $U_{e3}$  are the outputs of the fuzzy force tracking controller for the HA and the EHA, respectively, and can be determined from the fuzzy rules presented in Table 3.

The membership function for each parameter of the FFTC is given in Table 4.

The varied ranges of the parameters of the FFTC are bounded. A suitable range of each parameter was found by experiments. The range of each parameter for the FFTC is  $K_{ph} \in [4.7 \times 10^{-6}, 4.9 \times 10^{-6}]$ ,  $K_{ih} \in [1.18 \times 10^{-6}, 1.2 \times 10^{-6}]$ ,  $K_{dh} \in [1.9 \times 10^{-7}, 2.1 \times 10^{-7}]$ ,  $K_{pe} \in [0.097, 0.099]$ ,  $K_{ie} \in [1.98 \times 10^{-6}, 2 \times 10^{-6}]$ , and  $K_{de} \in [8.98 \times 10^{-3}, 9 \times 10^{-3}]$ . Eq. (12) is also used as the parameter adjustment mechanism for the FFTC.

Furthermore, there are two low pass filters at the output of the FFTC used to remove the noise in the signal. For  $I_{s3}$ , it is found that the noises are signals with a high frequency (20 Hz), while for  $U_{e3}$ , it is found that the noises are signals with a

**Table 2** Membership functions for the FPTC.

Parameters	Membership function														
	$e_p$					$\dot{e}_p$					$K'_p, K'_i$				
	NB	NS	ZE	PS	PB	NB	NS	ZE	PS	PB	S	MS	M	MB	B
$a_r$	-15	-10	-5	0	5	-75	-50	-25	0	25	0.1	0.15	0.30	0.5	0.7
$b_r$	-10	-5	0	5	10	-50	-25	0	25	50	0.15	0.3	0.5	0.7	1
$c_r$	-5	0	5	10	15	-25	0	25	50	75	0.3	0.5	0.7	1	1.15

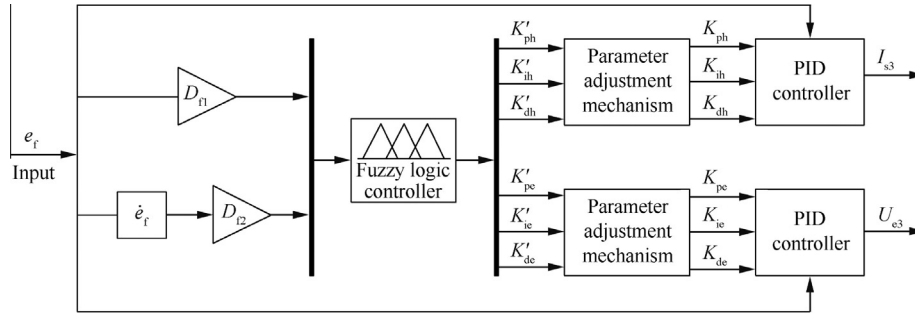


Fig. 10 Internal structure of fuzzy force tracking controller.

Table 3 Fuzzy rules for the FFTC.

Change of error $\dot{e}_f$	Error $e_f$				
	NB	NS	ZE	PS	PB
NB	M	MB	B	B	B
NS	MS	M	MB	MB	B
ZE	S	MS	M	MB	B
PS	S	MS	MS	M	MB
PB	S	S	S	MS	M

frequency above 79 Hz. Therefore, the gain of the low pass filter is  $K_f = 1$ . The transfer function of the low pass filter is given by

$$T(s) = \frac{K_f \omega_c^2}{s^2 + 2\zeta \omega_c s + \omega_c^2} \quad (13)$$

where  $\omega_c$  is the cut-off frequency;  $K_f$  is the passband or gain of the filter;  $\zeta$  is the damping factor.

#### 4. Simulation results and discussion

In order to verify the effectiveness of the proposed controller, this paper applies the control strategies of pursuit, rejection, and force equalization into MATLAB/Simulink by using the parameters shown in Table 5.

##### 4.1. Simulation results with a square wave load

In this simulation, a step demand (30 mm position signal) is sent at time 0 s with an external force of 15000 N. The external force is a square wave of a 2 s period with a 1 s phase delay and a 50% pulse width of the period and it acts on the surface from 1 s to 5 s. The simulation results are shown in Fig. 11.

It is noted that the maximum force fighting for the PID design strategy is 8350 N initial and there is no external force

at that time. The integrated fuzzy controller strategy has no initial force fighting. Then a 15 kN external load (force) acts on the control surface at a time of 1 s with a period of 2 s. It is observed that the force fighting for PID control is  $-6800$  N, while the force fighting for the integrated fuzzy controller strategy is  $-1400$  N at that time. It means that the proposed strategy has reduced 79.4% force fighting as compared to the PID strategy. Force fighting comparison of the proposed strategy with the PID strategy is given in Table 6.

Furthermore, it shows that the integrated fuzzy strategy has better synchronization. The proposed strategy also quickly follows the signal given by the desired trajectory as compared to the PID strategy as shown in Fig. 11(b). In addition, for PID, the load pressures of the HA and the EHA have a greater difference as shown in Fig. 11(c), which causes poor synchronization. The integrated fuzzy strategy has a less difference between the load pressures of the HA and the EHA as compared to the PID strategy as shown in Fig. 11(d).

##### 4.2. Simulation results with a sinusoidal wave load

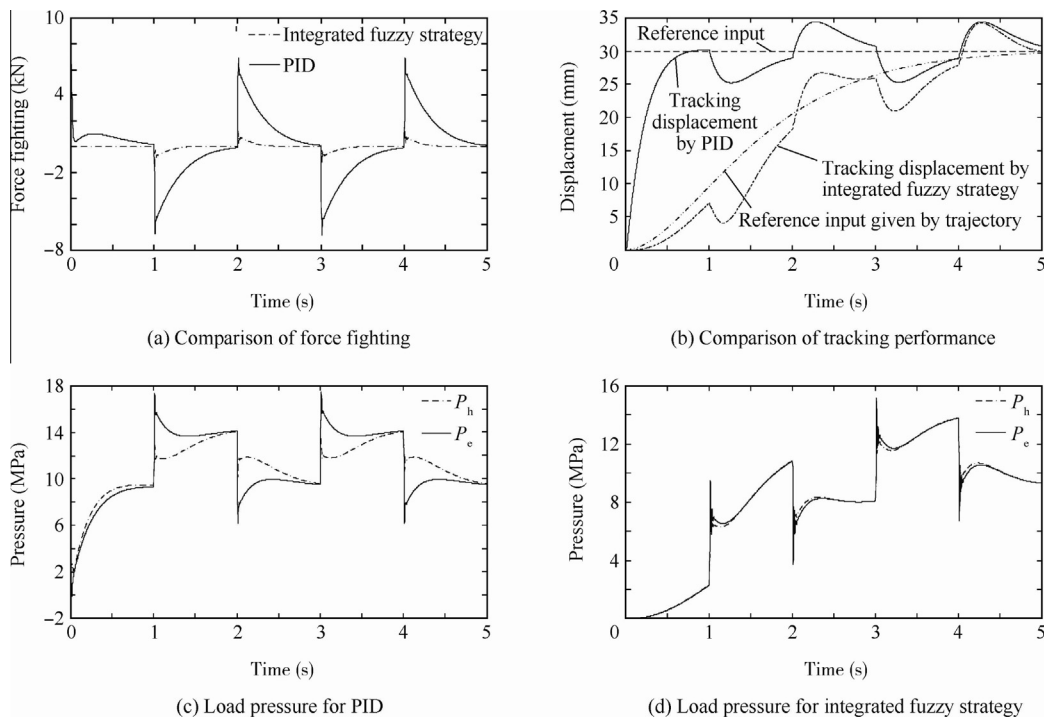
Suppose that the control surface of the aircraft (at a time of 1 s) experiences a disturbance (load) just like a sine wave of 15 kN in amplitude and 2 s in period. The simulation results are shown in Fig. 12.

It is noted that the maximum force fighting for the PID design strategy is 8350 N initial (at 0 s) and there is no external force at that time. The integrated fuzzy controller strategy has no initial force fighting. The force fighting when the external load acts on the control surface is  $-4430$  N for the PID strategy and it is  $-400$  N for the integrated fuzzy strategy. Comparison of force fighting is given in Table 7.

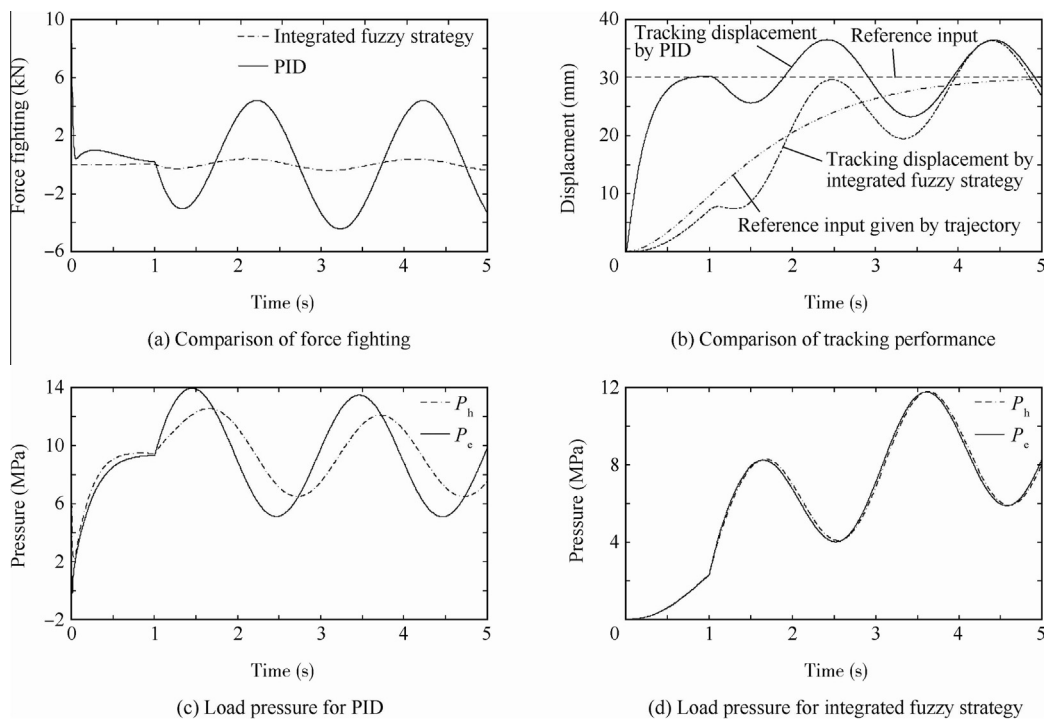
In this simulation, it also shows that the fuzzy integrated strategy has better synchronization than the PID strategy according to Fig. 12(b). For PID, the load pressures of the HA and the EHA have a greater difference as shown in

Table 4 Membership functions for the FFTC.

Parameters in membership function	Membership function																			
	$e_f$					$\dot{e}_f$					$K'_{ph}, K'_{ih}, K'_{dh}, K'_{ie}, K'_{de}$					$K'_{pe}$				
	NB	NS	ZE	PS	PB	NB	NS	ZE	PS	PB	S	MS	M	MB	B	S	MS	M	MB	B
$a_r$	-100	-10	-5	0	5	-100	-8	4	0	4	0.1	0.15	0.3	0.5	0.7	0.87	0.90	0.92	0.95	0.97
$b_r$	-10	-5	0	5	10	-8	-4	0	4	8	0.15	0.3	0.5	0.7	1	0.90	0.92	0.95	0.97	1
$c_r$	-5	0	5	10	100	-4	0	4	8	100	0.3	0.5	0.7	1	1.15	0.92	0.95	0.97	1	1.15



**Fig. 11** Simulation results with a square wave load.



**Fig. 12** Simulation results with a sine wave load.

Fig. 12(c), which causes poor synchronization. Compared to the PID strategy, the integrated fuzzy strategy has a less difference between the load pressures of the HA and the EHA as shown in Fig. 12(d).

Robustness is a property that shows how much system performance is sensitive to uncertainties (disturbances, variations in parameters, etc.). The PID strategy is not robust because it doesn't count the coupling effect. However, the integrated



**Table 5** Simulation parameters for the dissimilar redundant system.

Item	Parameter	Value
Servo valve	$K_i$ ( $\text{m}^{-1}\cdot\text{A}$ )	$3.04 \times 10^{-3}$
	$K_q$ ( $\text{m}^{-2}\cdot\text{s}$ )	2.7
	$K_c$ ( $\text{m}^3\cdot\text{s}^{-1}\cdot\text{Pa}^{-1}$ )	$1.75 \times 10^{-11}$
Motor pump	$L_e$ (H)	$3.36 \times 10^{-3}$
	$R_e$ ( $\Omega$ )	0.245
	$K_e$ ( $\text{V}\cdot\text{rad}^{-1}\cdot\text{s}$ )	0.215
	$J_m$ ( $\text{kg}\cdot\text{m}^2$ )	$1.6 \times 10^{-3}$
	$B_m$ ( $\text{N}\cdot\text{m}\cdot\text{rad}^{-1}\cdot\text{s}$ )	$6 \times 10^{-4}$
	$K_m$ ( $\text{N}\cdot\text{m}\cdot\text{A}^{-1}$ )	0.179
	$V$ ( $\text{m}^3\cdot\text{r}^{-1}$ )	$1 \times 10^{-6}$
Hydraulic cylinder	$A_h, A_e$ ( $\text{m}^2$ )	$1.47 \times 10^{-3}$
	$E_h, E_e$ (Pa)	$8 \times 10^8$
	$m_h, m_e$ (kg)	55
	$B_h, B_e$ ( $\text{N}\cdot\text{m}^{-1}\cdot\text{s}$ )	$1 \times 10^4$
	$V_h, V_e$ ( $\text{m}^3$ )	$1.47 \times 10^{-4}$
	$C_{hl}, C_{el}$ ( $\text{m}^3\cdot\text{s}^{-1}\cdot\text{Pa}^{-1}$ )	$1.0 \times 10^{-11}$
	Control surface	$K$ ( $\text{N}\cdot\text{m}^{-1}$ )
$K_d$ ( $\text{N}\cdot\text{m}^{-1}$ )		$9.14 \times 10^5$
$m_d$ (kg)		600
$B_d$ ( $\text{N}\cdot\text{m}\cdot\text{rad}^{-1}\cdot\text{s}$ )		2300

**Table 6** Comparison between strategies under a square wave load.

Control strategy	Force fighting (N)	
	Without load	With load
PID	8350	-6800
Integrated fuzzy	0	-1400

**Table 7** Comparison between strategies under a sine wave load.

Control strategy	Force fighting (N)	
	Without load	With load
PID	8350	-4430
Integrated fuzzy	0	-400

fuzzy controller strategy is robust because it counts the coupling effect and consists of feedback and feed-forward controllers to make the system fast with reduced errors.

## 5. Conclusions

In this paper, an integrated fuzzy controller design is proposed that consists of a trajectory generator, a position controller, and an FFTC. The trajectory generator is designed according to the dynamic characteristics of the EHA. The position controller combines the advantages of a feed-forward controller and a feedback controller to reduce force fighting and synchronize them by taking input signals from the trajectory generator. The FFTC improves load rejection performance and reduce dynamic force fighting by taking into account the

inherent coupling effect. Simulation results show that the proposed controller design strategy completely removes initial force fighting, while there is a very big improvement in eliminating force fighting. It is also shown that the load pressure difference is also smaller as compared to that of PID and the proposed strategy has better tracking performance.

## Acknowledgments

This work was supported by the National Basic Research Program of China (973 Program) (No. 2014CB046402), the National Natural Science Foundation of China (Nos. 51575019, 51305011), and the 111 Program of China.

## References

- Ahn KK, Nam DNC, Jin M. Adaptive backstepping control of an electrohydraulic actuator. *IEEE/ASME Trans Mechatron* 2014;**19**(3):987–95.
- Wang XJ, Wang SP. High performance adaptive control of mechanical servo system with lugre friction model: identification and compensation. *J Dyn Syst Meas Contr* 2012;**134**(1):011021.
- Yao B, Bu F, Reedy J, Chiu GT. Adaptive robust motion control of single-rod hydraulic actuators: theory and experiments. *IEEE/ASME Trans Mechatron* 2000;**5**(1):79–91.
- Goupil P. Airbus state of the art and practices on FDI and FTC in flight control system. *Control Eng Pract* 2011;**19**(6):524–39.
- Kang RJ, Jiao ZX, Wang SP, Chen LS. Design and simulation of electro-hydrostatic actuator with a built-in power regulator. *Chin J Aeronaut* 2009;**22**(6):700–6.
- Grabbel J, Ivantysynova M. An investigation of swash plate control concepts for displacement controlled actuators. *Int J Fluid Power* 2005;**6**(2):19–36.
- Li K, Lv Z, Lu K, Yu P. Thermal-hydraulic modeling and simulation of the hydraulic system based on the elec-tro-hydro-static actuator. *Procedia Eng* 2014;**80**:272–81.
- Lin Y, Shi Y, Burton R. Modeling and robust discrete-time sliding-mode control design for a fluid power electrohydraulic actuator (EHA) system. *IEEE/ASME Trans Mechatron* 2013;**18**(1):1–10.
- Tri NM, Nam DNC, Park HG, Ahn KK. Trajectory control of an electro hydraulic actuator using an iterative backstepping control scheme. *Mechatronics* 2014;**29**:96–102.
- Shi C, Wang XJ, Wang SP, Wang J, Tomovic MM. Adaptive decoupling synchronous control of dissimilar redundant actuation system for large civil aircraft. *Aerosp Sci Technol* 2015;**47**:114–24.
- Bauer C, Lagadec K, Bès C, Mongeau M. Flight control system architecture optimization for fly-by-wire air-liners. *J Guid Control Dyn* 2007;**30**(4):1023–9.
- Rosero J, Ortega J, Aldabas E, Romeral L. Moving towards a more electric aircraft. *IEEE Aerosp Electron Syst Mag* 2007;**22**(3):3–9.
- Yu LM, Ye ZQ. Research on performances of hybrid actuation system with dissimilar redundancies. *Adv Mater Res* 2012;**430–432**:1559–63.
- Ismail S, Pashilkar AA, Ayyagari R, Sundararajan N. Improved neural-aided sliding mode controller for auto-landing under actuator failures and severe winds. *Aerosp Sci Technol* 2014;**33**(1):55–64.
- Guo LL, Yu LM, Lu Y, Fan DL. Multi-mode switching control for HSA/EHA hybrid actuation system. *Appl Mech Mater* 2014;**494–495**:1088–93.
- Karam W, Mare JC. Force control of a rollerscrew electromechanical actuator for dynamic loading of aerospace actuators. *International conference on fluid power and motion control*; 2008. p. 515–28.

17. Cochoy O, Hanke S, Carl UB. Concepts for position and load control for hybrid actuation in primary flight controls. *Aerosp Sci Technol* 2007;**11**(2):194–201.
18. Wang LJ, Maré JC. A force equalization controller for active/active redundant actuation system involving servo-hydraulic and electro-mechanical technologies. *Proc Inst Mech Eng Part G J Aerosp Eng* 2014;**228**(10):1768–87.
19. Li TS, Tong SC, Feng G. A novel robust adaptive-fuzzy-tracking control for a class of nonlinear multi-input/multi-output systems. *IEEE Trans Fuzzy Syst* 2010;**18**(1):150–60.
20. Wang XJ, Wang SP, Zhao P. Adaptive fuzzy torque control of passive torque servo systems based on small gain theorem and input-to-state stability. *Chin J Aeronaut* 2012;**25**(6):906–16.
21. Li THS, Huang YC. Mimo adaptive fuzzy terminal sliding-mode controller for robotic manipulators. *Inf Sci* 2010;**180**(23):4641–60.
22. Wang XJ, Wang SP, Yao B. Adaptive robust torque control of electric load simulator with strong position coupling disturbance. *Int J Control Autom Syst* 2013;**11**(2):325–32.
23. Taher SA, Hematti R, Abdolalipour A, Nemati M. Decentralized controller design for static synchronous compensator using robust quantitative feedback theory method. *Am J Eng Appl Sci* 2008;**1**(1):66–75.
24. Jung JW, Leu VQ, Do TD, Kim EK, Choi HH. Adaptive PID speed control design for permanent magnet synchronous motor drives. *IEEE Trans Power Electron* 2015;**30**(2):900–8.
25. Benaskeur AR, Desbiens A. Backstepping-based adaptive PID control. *IEE Proc Control Theory Appl* 2002;**149**(1):54–9.
26. Chen KY, Tung PC, Tsai MT, Fan YH. A self-tuning fuzzy PID-type controller design for unbalance compensation in an active magnetic bearing. *Expert Syst Appl* 2009;**36**(4):8560–70.
27. Hu B, Mann GK, Gosine RG. New methodology for analytical and optimal design of fuzzy PID controllers. *IEEE Trans Fuzzy Syst* 1999;**7**(5):521–39.

**Waheed Ur Rehman** received his B.S. degree in mechatronics engineering from U.E.T Taxila, Pakistan in 2012 and is currently a Master's student at Beihang University, China. His current research is about control of hybrid systems, control of nonlinear mechatronics systems, etc.

**Wang Shaoping** received her Ph.D., M.E., and B.E. degrees in mechatronics engineering from Beihang University, China, in 1994, 1991, and 1988, respectively. She has been with the School of Automation Science and Electrical Engineering at Beihang University since 1994 and was promoted to the rank of professor in 2000. Her research interests are engineering reliability, fault diagnostic, prognostic and health management, as well as active fault tolerant control.

**Wang Xingjian** received his Ph.D. and B.E. degrees in mechatronics engineering from Beihang University, China, in 2012 and 2006, respectively. From 2009 to 2010, he was a visiting scholar in the School of Mechanical Engineering at Purdue University, West Lafayette, IN, U.S. He is currently with the School of Automation Science and Electrical Engineering at Beihang University, Beijing, China. His research interests are nonlinear control, active fault tolerant control, fault diagnostic, and fault prognostic.

**Fan Lei** received his M.S. degrees from PLA University of Science and Technology in 2011 and is currently a Ph.D. student at Beihang University, China. His current research is about fault diagnosis and reliability of mechatronics systems.

**Kamran Ali Shah** received his B.S. degree in electrical (telecom) engineering from CIIT Wah Cantt, Pakistan in 2013. He is currently a Master's student at Beihang University, having research interests in nonlinear control of power devices, etc.